



THE UNIVERSITY *of* EDINBURGH

Edinburgh Research Explorer

Differential protection of neuromuscular sensory and motor axons and their endings in Wld(S) mutant mice

Citation for published version:

Oyebode, ORO, Hartley, R, Singhota, J, Thomson, D & Ribchester, RR 2012, 'Differential protection of neuromuscular sensory and motor axons and their endings in Wld(S) mutant mice' *Neuroscience*, vol 200, pp. 142-158. DOI: 10.1016/j.neuroscience.2011.10.020

Digital Object Identifier (DOI):

[10.1016/j.neuroscience.2011.10.020](https://doi.org/10.1016/j.neuroscience.2011.10.020)

Link:

[Link to publication record in Edinburgh Research Explorer](#)

Document Version:

Peer reviewed version

Published In:

Neuroscience

General rights

Copyright for the publications made accessible via the Edinburgh Research Explorer is retained by the author(s) and / or other copyright owners and it is a condition of accessing these publications that users recognise and abide by the legal requirements associated with these rights.

Take down policy

The University of Edinburgh has made every reasonable effort to ensure that Edinburgh Research Explorer content complies with UK legislation. If you believe that the public display of this file breaches copyright please contact openaccess@ed.ac.uk providing details, and we will remove access to the work immediately and investigate your claim.



Differential protection of neuromuscular sensory and motor axons and their endings in *Wld^S* mutant mice

O. R. O. Oyebode,¹R. Hartley,¹J. Singhota, D. Thomson AND R. R. Ribchester*

Euan MacDonald Centre for Motor Neurone Disease Research, Hugh Robson Building, University of Edinburgh, George Square, Edinburgh EH8 9XD, UK

¹These authors contributed equally to this paper.

*Corresponding author. Tel: +44-131-650-3256; fax: +0131-650-3255. E-mail address: rrr@ed.ac.uk (R. R. Ribchester).

Abstract

Orthograde Wallerian degeneration normally brings about fragmentation of peripheral nerve axons and their sensory or motor endings within 24 – 48 h in mice. However, neuronal expression of the chimaeric, *Wld^S* gene mutation extends survival of functioning axons and their distal endings for up to 3 weeks after nerve section. Here we studied the pattern and rate of degeneration of sensory axons and their annulospiral endings in deep lumbrical muscles of *Wld^S* mice, and compared these with motor axons and their terminals, using neurone-specific transgenic expression of the fluorescent proteins yellow fluorescent protein (YFP) or cyan fluorescent protein (CFP) as morphological reporters. Surprisingly, sensory endings were preserved for up to 20 days, at least twice as long as the most resilient motor nerve terminals. Protection of sensory endings and axons was also much less sensitive to *Wld^S* gene-copy number or age than motor axons and their endings. Protection of γ -motor axons and their terminals innervating the juxtaequatorial and polar regions of the spindles was less than sensory axons but greater than α -motor axons. The differences between sensory and motor axon protection persisted in electrically silent, organotypic nerve-explant cultures suggesting that residual axonal activity does not contribute to the sensory-motor axon differences *in vivo*. Quantitative, *Wld^S*-specific immunostaining of dorsal root ganglion (DRG) neurones and motor neurones in homozygous *Wld^S* mice suggested that the nuclei of large DRG neurones contain about 2.4 times as much *Wld^S* protein as motor neurones. By contrast, nuclear fluorescence of DRG neurones in homozygotes was only 1.5 times brighter than in heterozygotes stained under identical conditions. Thus, differences in axonal or synaptic protection within the same *Wld* mouse may most simply be explained by differences in expression level of *Wld* protein between neurones. Mimicry of *Wld^S*-induced protection may also have applications in treatment of neurotoxicity or peripheral neuropathies in which the integrity of sensory endings may be especially implicated.

Key words: Wallerian degeneration, axon, muscle spindle, sensory neurone, motor neurone, neuromuscular junction.

There is growing evidence that degeneration of axon terminals precedes death of cell bodies in several forms of neurodegenerative disease (Selkoe, 2002; Gillingwater et al., 2003; Forero et al., 2006; Lin and Koleske, 2010). For example, in amyotrophic lateral sclerosis (ALS), some motor nerve terminals become sensitive to metabolic stress and degenerate before their cell bodies show overt pathological signs, both in humans with ALS and in mouse models of the disease (Frey et al., 2000; Fischer et al., 2004; Schaefer et al., 2005; David et al., 2007). Understanding the determinants and mechanisms of degeneration of axons and their terminals may therefore reveal molecular targets for mitigation of synaptopathies, axonopathies and other forms of neurodegenerative disease. An attractive, classic model of axonopathy is ‘Wallerian’ degeneration. Following nerve transection or other forms of local axonal trauma, the isolated distal compartments of neurones undergo active, orthograde degeneration. Fragmentation of distal axons, an early pathological sign of Wallerian degeneration, occurs about 36 h after nerve injury (Beirowski et al., 2004, 2005; Coleman and Freeman, 2010). Remarkably, however, degeneration of motor nerve terminals – the most distal components of the axon – is complete about 12–18 h earlier than this, that is, within 12–24 h of axotomy (Slater, 1966; Miledi and Slater, 1968; Winlow and Usherwood, 1975, 1976; Wong et al., 2009). Thus, Wallerian degeneration of some neuromuscular synaptic terminals is complete before more proximal parts of their axons may show any overt pathological signs (Gillingwater and Ribchester, 2001; Beirowski et al., 2004).

Surprisingly, following axonal trauma in *Wld^S* (‘Wallerian Degeneration – Slow’) mutant mice, some distal axons survive nerve injury for more than 3 weeks (Lunn et al., 1989; Mack et al., 2001; Beirowski et al., 2005, 2009). The spontaneous mutation responsible therefore confers one of the strongest neuroprotective phenotypes, selective for axons, yet discovered. Positional cloning and sequencing established that the mutation in *Wld^S* mice comprises an autosomal-dominant tandem triplication of a genomic DNA fragment of 85 kb. The fusion boundaries bridge the complete sequence of one native gene (*Nmnat-1*) and the partial, N-terminal sequence of another (*Ufd2*, now referred to as its mammalian homologue *Ube4b*) (Lyon et al., 1993; Coleman et al., 1998; Conforti et al., 2000). Transgenic expression of this chimaeric candidate gene confirmed its strong neuroprotective phenotype (Mack et al., 2001; Adalbert et al., 2005; Hoopfer et al., 2006; MacDonald et al., 2006; Martin et al., 2010). Both principal components of the *Wld^S* protein contain short peptide sequences that are necessary for axon protection, including the catalytic site for *Nmnat* enzymic activity and a valosin-containing peptide-binding motif in the N-terminus of *Ube4b* (Conforti et al., 2009). A nuclear localisation signal (NLS) embedded in *Nmnat-1* results, as expected, in strong intranuclear transport of *Wld^S* protein (Mack et al., 2001; Wilbrey et al., 2008). However, recent studies show that either inhibition of nuclear localisation of *Wld^S* or targeting low levels of cytoplasmic *Nmnat* activity to an intraxonal compartment, result in strengthening of both axonal and synaptic protection and counteract its age-dependence (Gillingwater et al., 2002; Beirowski et al., 2009; Babetto et al., 2010; Coleman and Freeman, 2010; Gilley and Coleman, 2010).

Thus, at least two variables determine the amount and extent of protection by *Wld^S* protein: its expression level and the proportion localised to intracellular components of the axon. In that context, we have re-examined the differences in protection reported previously between sensory and motor axons in *Wld^S* mice (Brown et al., 1994). First, we found that sensory-motor differences in *Wld^S*-induced axonal protection extend to the axon terminals. The annulospiral sensory endings innervating muscle spindles are protected for at least twice as long as the terminals of motor axons. Second, we show that axotomised sensory endings and axons remain responsive to peripheral stimulation and competent to conduct action potentials for several days. However, we found that differences in protection of sensory and motor axons persisted in quiescent, organotypic nerve explant culture, suggesting that differences in residual activity *in vivo* do not account for the differences in sensory/motor axon degeneration. Third, quantitative estimates of *Wld^S* immunostaining indicated stronger labelling of the largest neurones in the dorsal root ganglion (DRG) than in spinal motor neurones, suggesting that the overall level of *Wld^S* protein expression is

substantially greater in these DRG neurones than motor neurones. Taken together, the data indicate that the differences in protection of sensory and motor axons and their endings in *Wld^S* mice is most simply explained by differences in the overall amount of expression of *Wld^S* protein in sensory and motor neurones and their axonal branches. The robust protection of sensory axons and terminals we studied here underscores the therapeutic potential for mimicry of *Wld^S*-induced neuroprotection as a treatment for sensory neuropathies, in addition to motor axonopathies like ALS.

Animals

Mice from *thy-1.2XFP* (X=Y, yellow fluorescent protein; X=C, cyan fluorescent protein) lines (Jackson laboratories, Bar Harbor, USA) were mated with *Wld^S* homozygotes (Harlan-Olac, Sharnlow, UK) to produce *thy-1.2XFP: Wld* heterozygote lines. Back-crossing to *Wld^S* homozygotes produced *Wld^S* homozygotes that also expressed fluorescent protein in neurones. Mice of each genotype and at a range of ages between 8 and 88 weeks were examined for this study. All animal husbandry and surgical procedures were carried out in accordance with UK Home Office regulations

Surgery

Mice were anaesthetised by inhalation of halothane (Merial Animal Health Ltd., Harlow, UK) at 2–5% in oxygen and nitrous oxide (1:1). The sciatic nerve on one side was exposed by blunt dissection and approximately 1 mm of the nerve was removed. The skin wound was normally closed with a single suture using 7/0 silk thread with an integrated needle (Ethicon, Kirkton, UK), and the animals were returned to their cages and allowed to recover

Lumbrical muscle spindle dissection and analysis

We studied 65 lumbrical muscle spindles *in situ* and 15 teased spindles. Mice were sacrificed between 8 h and 20 days after the sciatic nerve cut, and the four deep lumbrical (DL) muscles from each hind foot were dissected in oxygenated mammalian physiological solution with mM concentrations as follows: NaCl 120; KCl 5; CaCl₂ 2; MgCl₂ 1; NaHCO₃ 23.8; D-glucose 5.6. Dissected preparations were incubated with α-bungarotoxin conjugated with tetramethylrhodamine isothiocyanate (TRITC-α-BTX; purchased from either Molecular Probes or Cambridge Bioscience, Cambridge, UK) for 10 min followed by washes in physiological solution, then fixed in 4% paraformaldehyde (PFA; Fisher Scientific, Loughborough, UK) for 20 min and finally washed in 1% phosphate buffered saline (1% PBS with the following millimolar concentrations; NaCl 137, KCl 2.76, Na₂HPO₄ 8.10 and KH₂PO₄ 1.47). In some preparations, muscle spindles were teased out of the lumbrical muscles, on a microscope slide in glycerol using a pair of pin vices before mounting. The position of the spindle was monitored using a compound fluorescence microscope during the dissection. Once the intrafusal muscle fibres were exposed to the extent that their innervation was distinct from all the extrafusal innervation, preparations were then mounted on glass slides in either Mowiol (Calbiochem, Nottingham, UK) or glycerol with 2.5% 1, 4-diazabicyclo [2.2.2] octane (DABCO) and covered with glass coverslips, to allow visualisation using fluorescence and confocal microscopy. Images were made using conventional fluorescence (Olympus BX50WI; Southend-on-Sea, UK, fitted with Hamamatsu C5810 (Welwyn Garden City, UK) or C4742-80 digital cameras and digitised using Perkin-Elmer/Improvision Openlab software, Seer Green, UK) or confocal microscopy (BioRad, Welwyn Garden City, UK; Radiance 2000 on a Nikon Eclipse E600 microscope, Kingston, UK). Some confocal stacks were subsequently volume rendered using Bitplane Imaris software (Bitplane Imaris, Zurich, Switzerland) (Supplementary Videos 1 and 2).

Electrophysiology

Mice were terminally anaesthetised with ketamine and xylazine and positioned on a platform that permitted exposure and extra-cellular recording with platinum wire electrodes from the exposed tibial nerves in the lower limb. Action potentials evoked by natural stimulation of the foot and ankle (touch, pressure, extension and flexion) were filtered and amplified (Neurolog, Digitimer, Welwyn

Garden City, UK) and recorded onto a PC using Spike-2 software via a CED1401+ interface (Cambridge Electronic Design, Cambridge, UK).

Vital staining of sensory endings

Lumbrical muscles were dissected as described previously. Muscles were then pinned in the Sylgard-coated (Dow Corning, Midland, USA) Petri dish and incubated with the fixable, vital aminostyryl dye FM1-43fx (Invitrogen, Paisley, UK) diluted in oxygenated physiological solution to give a final concentration of 4–10 μ M (Bewick et al., 2005). The muscles were pinned under full tension for 20 min and then returned to resting length for a further 20 min. This stretch followed by a relaxation of the muscles was repeated three times giving a total time of submersion in the FM1-43fx of 2 h. The solutions were continuously stirred by placing the dish on a rotating platform during incubations. Muscles were quickly washed in three changes of oxygenated physiological solution then fixed in 4% PFA for 20 min, then mounted in DABCO and glycerol.

Nerve explant culture

Dorsal root, ventral root, saphenous nerve and quadriceps nerve explants were dissected from mice killed by cervical dislocation and immediately placed in 3 ml of Dulbecco's Modified Eagle's Medium (DMEM) supplemented with Glutamax, 10% fetal bovine serum, 2-mM L-glutamine, 100 U/ml penicillin and 100 μ g/ml streptomycin (Gibco, Invitrogen) and cultured at 37 °C in 5% CO₂ for up to 15 days. After incubation the explants were rinsed in PBS for 5 s then fixed in fresh, buffered 4% PFA for 30 min. They were then mounted on slides with Tris buffered mounting media containing Mowiol and 2.5% DABCO.

Immunostaining of spinal cord and DRG

Mice were terminally anaesthetised with isoflurane and perfused transcardially with buffered 4% PFA (Electron Microscopy Sciences, Hatfield, PA, USA). A dorsal laminectomy exposed the spinal cord to allow free exchange of fluid then the preparation was immersed in PFA overnight. The cord with intact DRGs was removed and segments with DRGs (approximately 5 mm) were embedded in 6% low melting temperature agarose (NuSieve, Lonza, Basel, Switzerland). Transverse 100- μ m vibratome sections or whole DRG were incubated in blocking solution (4% BSA and 1% Triton X100 in PBS) for 2 h then with rabbit anti-Wld18 antibody (generous gift from Dr. M.P. Coleman, Babraham, UK) for 36 h in blocking solution at 4 °C. Sections were then washed for 20 min in PBS containing 1% Triton X100. They were then reincubated in blocking buffer for 1 h before overnight in 1/100 TRITC- or fluorescein isothiocyanate (FITC)-conjugated swine anti-rabbit secondary antibodies (DAKO, Ely, UK) in blocking buffer. Sections were washed for 20 min in PBS containing 1% Triton X100 and Tris buffer (pH 8.5) then mounted in Mowiol-DABCO antifade. Images and z-series were obtained using a Zeiss 710 confocal microscope (Welwyn Garden City, UK). Data are given as mean \pm SEM unless indicated otherwise.

Results

Annulospiral sensory and γ -fusimotor innervation of mouse lumbrical muscles

XFP mice crossbred with *Wld^s* mice (see Methods) show strong expression of cyan or yellow fluorescent protein in cell bodies, axons and the terminals of both sensory neurones and α -motor neurones innervating the deep lumbrical muscles (Fig. 1). Most lumbrical muscles also contained either one or two XFP-labelled spindles. Some contained three or more spindles; occasionally we were unable to locate any spindles in a lumbrical muscle. There was no difference or bias in the mean number of spindles in muscles of either foot, or with age, or gender (Oyebode, 2009).

Innervated muscle spindles viewed after microdissection from unoperated mouse DL muscles contained between two and five intrafusal muscle fibres, each less than 10 μ m in diameter, as described in other mouse muscles (Tourtellotte et al., 2001; Desaki et al., 2010) or rat lumbrical muscles (Porayko and Smith, 1968; Ovalle, 1972; Gates et al., 1991; Kucera et al., 1991). Each spindle was supplied by one large primary afferent axon, penetrating the capsule and terminating in annulospiral endings that wrapped the equatorial region of the intrafusal muscle fibres (Fig. 1, Supplementary Movie 1). Occasionally a second, smaller diameter axon innervated the same region. The length of the primary ending was $142.5 \pm 43.11 \mu$ m (mean \pm SEM, $n=80$). The median number of annulospiral rotations was between 22 and 23. There was no significant difference in either the length or number of spiral bands in lumbrical muscle spindles of mice aged 8–60 weeks (Oyebode, 2009). Fluorescent protein was also strongly expressed in the fusimotor, γ -innervation of thy1.2-YFP16 mouse lumbrical muscles (Fig. 1C). This comprised between two and five axons whose endings were distributed over the juxta-equatorial and polar regions, forming synapses on small motor endplates that stained positive for TRITC- α -bungarotoxin, thus marking them as neuromuscular nicotinic cholinergic synapses. Occasionally, one of the fusimotor axons also supplied a few (<5) collateral nerve branches to endplates on extrafusal muscle fibres. By convention, we refer to these as f3-motor axons (Porayko and Smith, 1968; Barker et al., 1977). Interestingly, no fusimotor axonal fluorescence was observed in unoperated thy1.2CFP mouse lumbrical muscles, despite the original report that all motor neurones express cyan fluorescent protein (CFP) in this line (Feng et al., 2000). Thus, counterstaining with TRITC- α -bungarotoxin of spindles dissected from these muscles showed only postsynaptic endplates with no overlying CFP-positive axon terminals.

Sensory innervation in *Wld^S* mice is more strongly protected from Wallerian degeneration than motor innervation

As we reported previously, in young adult (up to 8-weeks old) homozygous *Wld^S* mice, intramuscular motor axons and their terminals were preserved for at least 3 days after axotomy (Fig. 1D, E). By 5–7 days, only about 50% of motor endplates retain contact with motor nerve terminals and many of these endplates are only partially occupied (Gillingwater et al., 2002). In heterozygotes, degeneration of almost all motor terminals occurs within 12–36 h of axotomy, as in wild-type mice (Wong et al., 2009). Surprisingly, sensory axons and their annulospiral endings were well preserved for at least 5 days after axotomy in both homozygous and heterozygous *Wld^S* mice (Fig. 1F), and some annulospiral endings were still present in

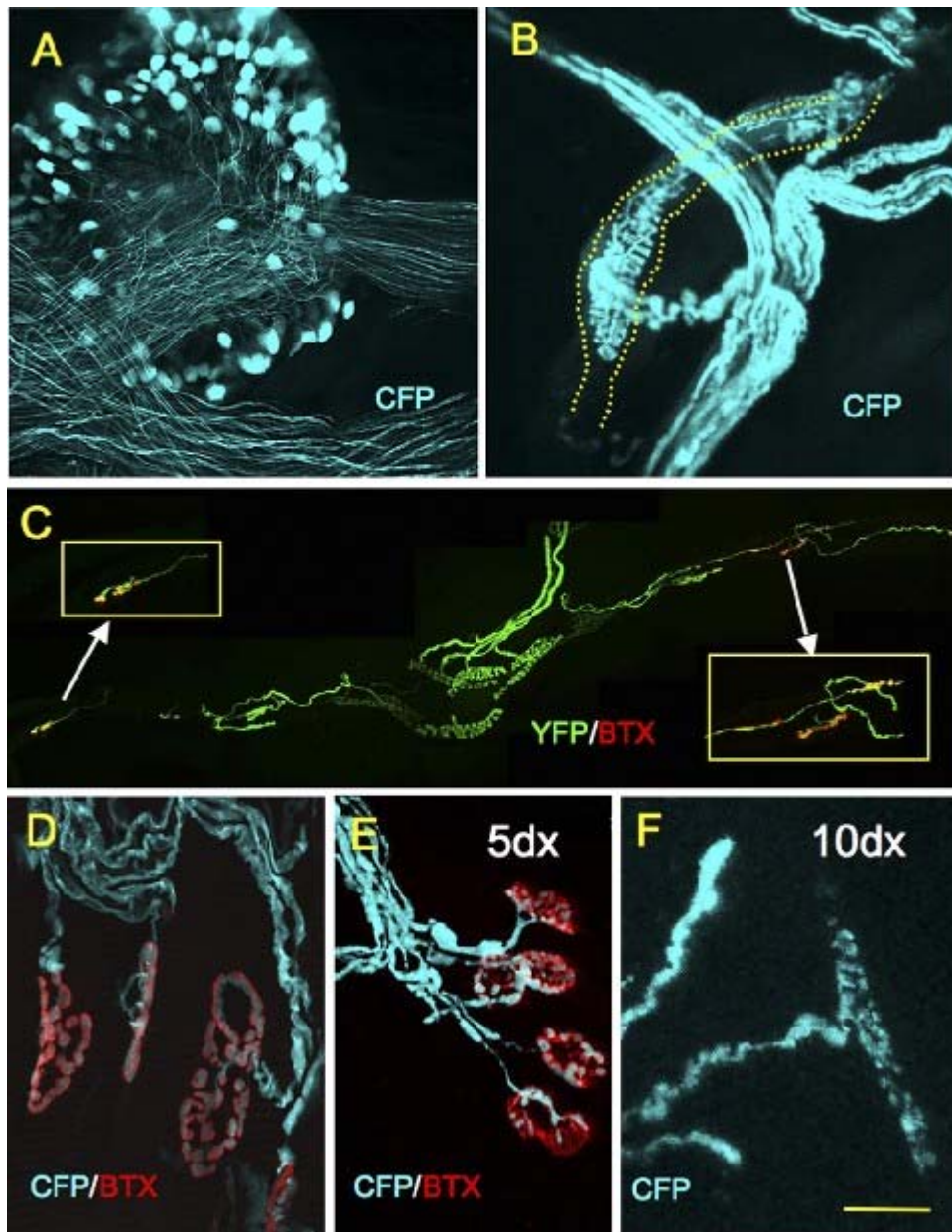


Fig. 1. Sensory neurons express thy1.2:YFP. (A) Whole mount preparation of a dorsal root ganglion from a thy1.2-CFP-expressing mouse, showing DRG neuronal cell bodies and axons. (B) Whole mount preparation of innervated lumbrical muscle showing axons, annulospiral ending supplied by a large primary afferent axon terminating on intrafusal muscle fibres (dotted outline). (C) Teased lumbrical muscle spindles from a thy1.2-YFP16 mouse, showing sensory and γ -motor axons innervating intrafusal neuromuscular junctions, counterstained in red with TRITC-a-bungarotoxin. (D) Neuromuscular junctions in unoperated thy1.2-CFP mice, counterstained with TRITC-a-bungarotoxin. (E) Neuromuscular junctions in *Wld^S* mouse lumbrical muscle 5 d after axotomy. (F) Preserved sensory axons and annulospiral endings in *Wld^S* mouse lumbrical muscle 10 d after axotomy. Calibrations: (A), 300 1-m; (B), 30 1-m; (C), 100 1-m; (D), 20 1-m; (E), 50 1-m; (F), 30 1-m. For interpretation of the references to color in this figure legend, the reader is referred to the Web version of this article.

axotomised DL muscles up to 20 days after axotomy, about 10 days longer than we have ever previously observed for axotomised motor nerve endings in *Wld^S* mice. As we reported previously, intramuscular axons and motor nerve terminals are only weakly protected in *Wld^S* mice older than about 4 months and most muscles lose all their motor innervation in these mice within 5 days of axotomy (Gillingwater et al., 2002; Beirowski et al., 2009). We were therefore surprised also to

observe strong preservation of sensory axons and endings in *Wld^S* mice older than 4 months (Fig. 2A–C; Supplementary Movie 2). In the oldest mouse we studied 5 days post axotomy (an 88-week-old *Wld^S* homozygote), no motor nerve terminals or intramuscular motor axons were preserved but four innervated spindles supplied by intact sensory axons remained altogether, in the four DL muscles of one hind foot.

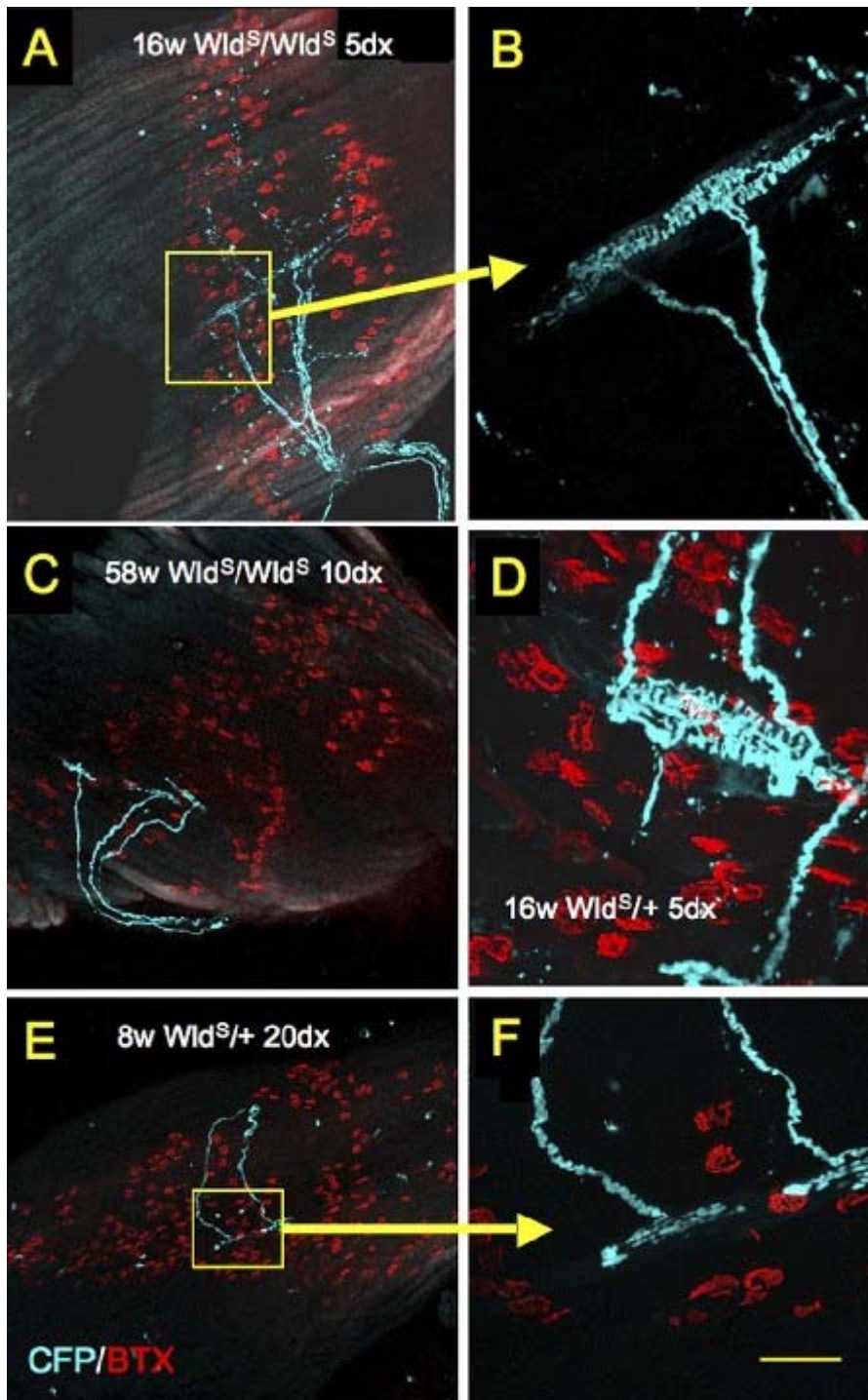


Fig. 2. Sensory axons and their annulospiral endings are better preserved than motor axons in aged and heterozygous thy1.2-CFP: *Wld^S* mice. All skeletomotor innervation had degenerated in these muscles, as indicated by staining of unoccupied motor endplates with TRITC- α -bungarotoxin, whereas the primary afferent axons and their intrafusal endings, as indicated by persistent CFP fluorescence, were largely intact. (A) 16-wk-old *Wld^S* homozygote 5 d after tibial nerve section. (B) Higher magnification of the ending outlined (yellow

box) in (A). (C) 58-wk-old *Wld^S* homozygote, 10 d after tibial nerve section. (D) 16-wk-old *Wld^S* heterozygote, 5 d axotomised. (E) 8-wk-old heterozygote, axotomised 20 d. (F) Higher magnification of the ending outlined (yellow box) in (E). Calibrations (bar in F): (A), 200 μ m; (B), 50 μ m; (C), 200 μ m; (D), 30 μ m; (E), 200 μ m; (F), 50 μ m. For interpretation of the references to color in this figure legend, the reader is referred to the Web version of this article.

The number of muscle spindles with sensory innervation did not change significantly up to 5 days post axotomy in wild-type mice but was significantly reduced by 20 days post axotomy in *Wld^S* homozygotes but was significantly reduced by 20 days post axotomy in *Wld^S* heterozygotes. However, the number of annulospiral bands decreased from about 22 to about 12 within 5 days and was reduced to about 5 annuli per spindle by 10 days (Fig. 3C), suggesting that axotomy-induced degeneration of sensory endings occurred by intercalary breakdown of the terminal structures. There was also no significant difference in the number of spindles with preservation of sensory innervation comparing *Wld^S* /+ heterozygotes with *Wld^S* homozygotes at any age (Fig. 3D). Like motor axons, we also occasionally noted instances of

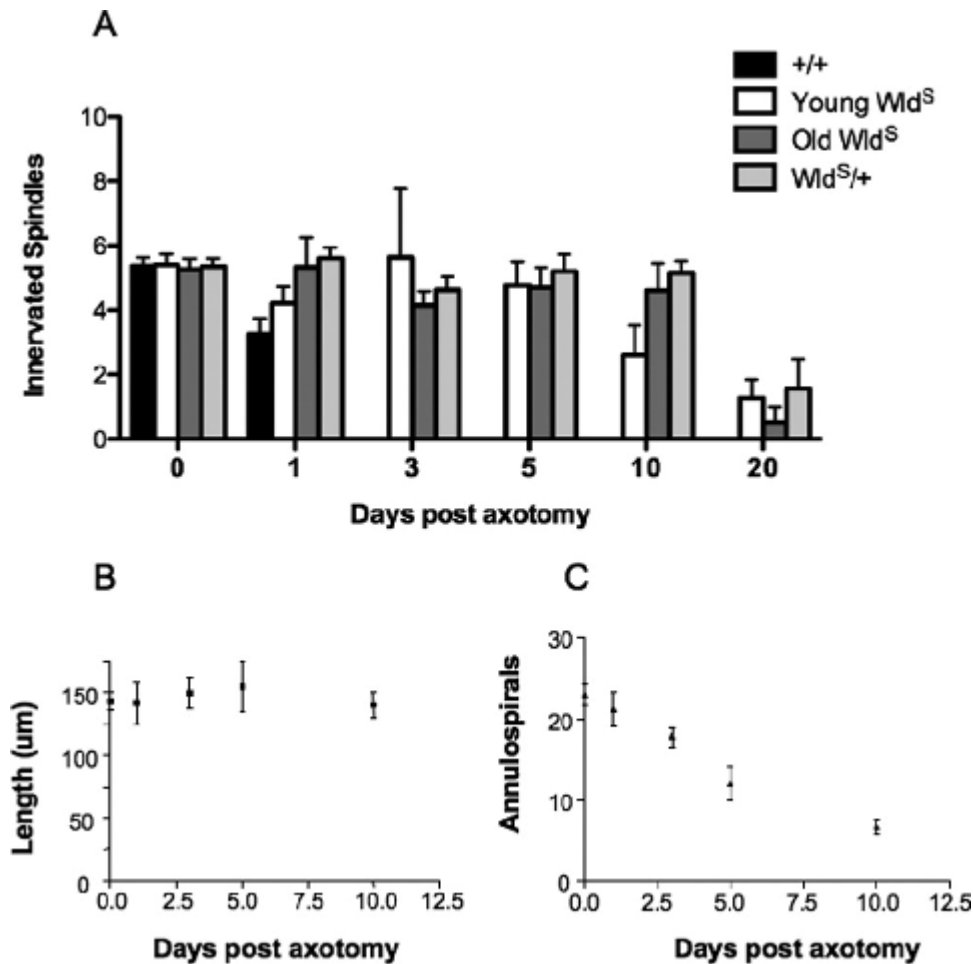


Fig. 3. Morphological analysis of the sensory innervation of muscle spindles in wild-type and *Wld^S* mice. (A) Afferent terminals degenerated 24 – 48 h after axotomy in wild-type (+/+) mice but persisted for up to 20 d in axotomised *Wld^S* mouse lumbrical muscles. The number of innervating sensory axons persisting in axotomised *Wld^S* muscles was insensitive to either age or mutant gene copy number, comparing young adult homozygotes ('Young *Wld^S*'; 1–2 mon), old homozygotes ('Old *Wld^S*', >6 mon of age), or young heterozygotes (*Wld^S/+*). (B) There was no change in the overall length of annulospiral endings in *Wld^S* mouse muscle after axotomy, at least for 10 d; but (C) the number of annulospiral rotations steadily reduced from 1–10 d after axotomy. All data shown are mean \pm SEM.

creased from about 22 to about 12 within 5 days and was reduced to about 5 annuli per spindle by 10 days (Fig. 3C), suggesting that axotomy-induced degeneration of sensory endings occurred by intercalary breakdown of the terminal structures. There was also no significant difference in the number of spindles with preservation of sensory innervation comparing *Wld^S* /+ heterozygotes with *Wld^S* homozygotes at any age (Fig. 3D). Like motor axons, we also occasionally noted instances of

sensory axons ending bluntly in the vicinity of muscle spindles, presumably because their endings had completely degenerated in advance of the axon (Oyebode, 2009).

Therefore, muscle spindles in *Wld^S* mice remain innervated by sensory axons and their endings more than 10 times longer than they do in wild-type mice after nerve injury and more than twice as long as intramuscular skeletal motor axons innervating the same muscles. Most notably, this additional protection appears to be much less age-dependent and less sensitive to *Wld^S* gene-copy number than degeneration of motor nerve terminals.

Does the neuroprotective effect of *Wld^S* depend on axonal branching?

Recent studies indicate that the neuroprotective effect of *Wld^S* protein is determined by its presence in the axon, in very low abundance, rather than via the nucleus, where the protein is normally highly abundant (Mack et al., 2001; Wilbrey et al., 2008). If the amount and distribution of *Wld^S* protein in axons determines its neuroprotective strength and if the amount of *Wld^S* synthesised by different neurones were similar, then we might expect nerve branching to dilute its downstream effects. By comparison, we know that the protective effect of the *Wld^S* gene is reduced in heterozygotes, in which the level of *Wld^S* protein expression is approximately half that of homozygotes (Mack et al., 2001; Conforti et al., 2007, 2009). This hypothesis would predict that axons with the fewest branches would be the most strongly protected, and neurones with the most extensive distal axonal branching would be the least protected. Connectomic analysis (Lu et al., 2009) of mouse

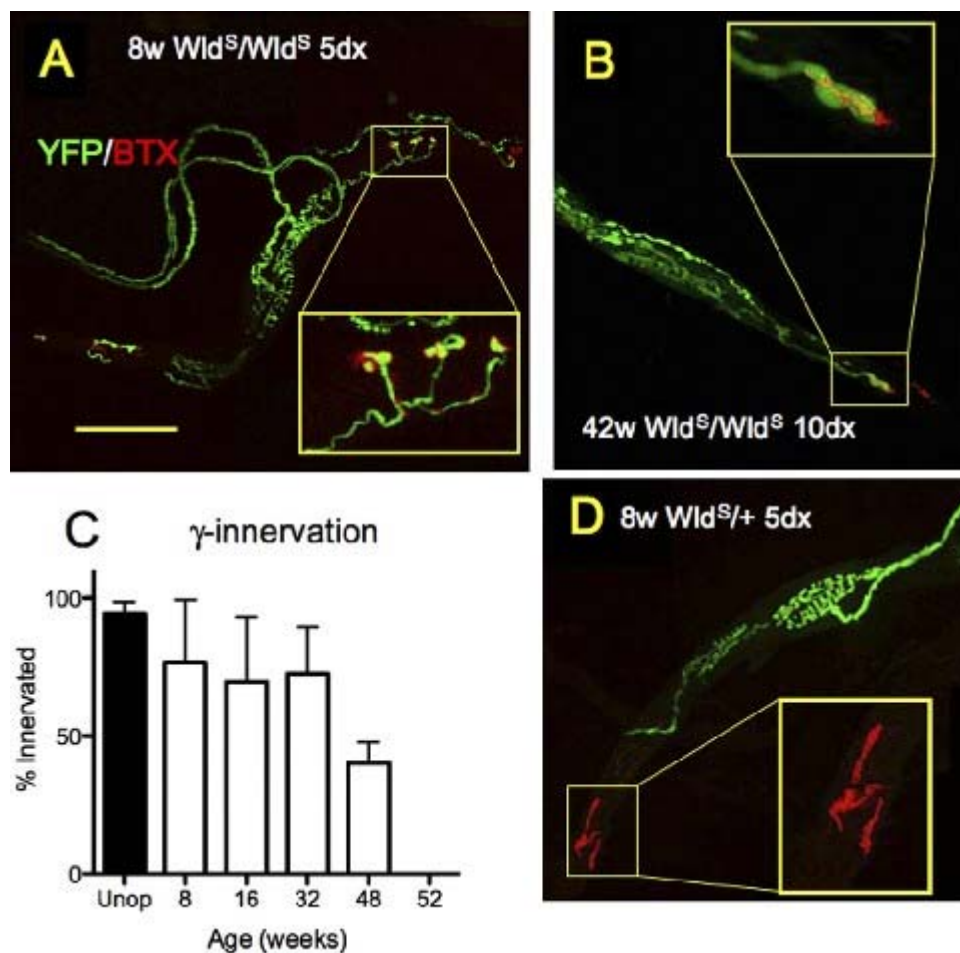


Fig. 4. Gamma motor innervation is partially preserved in old *Wld^S* homozygotes but not heterozygous mice. Teased muscle spindle preparation showing persistent sensory and γ -motor axons and their terminals in (A) an 8-wk-old thy1.2-YFP16:*Wld^S* homozygous mouse lumbrical, 5 d after axotomy. (B) 42-wk-old *Wld^S* homozygote 10 d post axotomy. (C) Summary of quantitative data (mean \pm SEM) obtained on persistent

innervation motor innervation, 5 d post axotomy in homozygous *Wld^S* mice up to 52 wks of age. (D) No fusimotor -γ-innervation (0%) persisted 5 d post axotomy in lumbrical muscles of heterozygous 8-wk-old *Wld^S* mice. Teased spindle for a thy1.2-YFP16:*Wld^S* heterozygote, showing persistence of sensory but not motor innervation. The degeneration of the motor terminals is indicated by vacant, TRITC-α-BTX staining (red) of the intrafusal motor endplates. Calibration: 50 μm. For interpretation of the references to color in this figure legend, the reader is referred to the Web version of this article.

lumbrical muscles shows they contain about 250 – 450 extrafusal muscle fibres, and these are normally innervated by four to eight motor axons, with skewed distribution of motor unit sizes, normally between about 10 and 60 muscle fibres. The mean motor unit size is about 40 muscle fibres (Gillingwater et al., 2002; Teriakidis et al., unpublished data). In addition, the relative volume of the axonal compartment of motor neurones is about 30 times the volume of the cell soma; and the volume of the branched, intramuscular axonal compartment is about four times that of the soma (Ribchester and Hartley, unpublished data). Thus, reducing intramuscular axonal branching by, say, 80% would reduce the total cytoplasmic/axoplasmic volume by less than 10% (and therefore minimally affecting the total amount of *Wld^S* protein present) but could radically increase the level of neuroprotective agent in each intramuscular collateral axon branch. The extent of nerve branching in either -γ- or f3-innervated spindles is about 5–25 times less than in motor units supplied by α-motor axons. Thus, to evaluate the hypothesis that dilution of the neuroprotective effect may be related to axonal branching, we measured the degeneration of the fusimotor innervation in thy1.2-YFP16: *Wld^S* mice. Seven teased spindles from seven 8-week-old thy1.2-YFP16: *Wld^S* homozygotes, sacrificed 5 days post axotomy, showed protection of the -γ-innervation of the intrafusal muscle fibres (Fig. 4A). The percentage of innervated-γ-endplates on muscle spindles from *Wld^S* mice 5 days post axotomy was not significantly different from the percentage of innervated -γ-endplates in teased spindles from unoperated mice ($P=0.4051$ Mann–Whitney U -test). Teased spindles from older *Wld^S* mice, including seven from mice aged 42 weeks, showed -γ-innervation 5–10 days post axotomy. In addition, three out of six teased spindles from mice aged 42 weeks showed some -γ-innervation at 10 days post axotomy (Fig. 4B). Overall, there was no significant difference in the percentage innervation of the -γ-endplates comparing teased spindles from unoperated mice and teased spindles from *Wld^S* mice 5 days post axotomy, in any of the 8-week-, 16-week- or 32-week-old age groups we studied (Dunn's Multiple Comparison test; Fig. 4C). However, there was a significant difference between the percentage innervation of -γ-endplates in 42-week-old *Wld^S* animals, 5 days post axotomy, and from unoperated spindles ($P<0.05$ Dunn's Multiple Comparison test). Teased spindles from mice aged 58 weeks showed no -γ-innervation at either 3 days or 5 days ($n=7$ in each case) post axotomy.

By contrast, teased spindles from *Wld^S* heterozygotes showed no -γ-innervation at all at either 3 ($n=7$), or at 5 days post axotomy ($n=6$; Fig. 4C, D). This rapid rate of degeneration was therefore indistinguishable from that of α-motor endings in heterozygous *Wld^S* mice (Wong et al., 2009). Taken together, these data suggest that -γ-innervation is preserved by *Wld^S* at ages when protection of α-motor innervation is no longer robust, suggesting that intramuscular axonal branching does contribute to the differences in protection of intramuscular axons, collateral branches and their terminals. However, the degree of protection of -γ-fusimotor innervation was evidently just as sensitive to gene-copy number as that of α-motor units, suggesting a non-linear dependence of protection on concentration of protective agent. In neither case was protection as robust as sensory innervation. It may be that axonal branching is a weak modifier of the strength of protection conferred by the *Wld^S* gene and the effect of dilution of the mediator is influential, but not decisive in determining the strength of the phenotype. However, there may be other differences between these different neuronal types and the levels of *Wld^S* protein they express, which may further contribute to the differences in protection of sensory, skeletomotor and fusimotor axons, and their terminals.

Other possible determinants of slow sensory axonal degeneration

In seeking a clear explanation for the sensory-motor differences in protection, we next considered whether differences in residual activity in the distal stumps, or whether differences in expression or localisation of *Wld^s* protein might be contributory or decisive factors. The results showed later in the text suggest that activity probably plays no role but differences in expression levels of *Wld^s* protein may provide a sufficient explanation.

Axotomised sensory endings are functional in vivo and in vitro. We tested first whether axotomised distal sensory (afferent) axons in *Wld^s* mice show persistent endogenous residual activity. Propagated centripetal (efferent) motor activity terminates at the site of a peripheral nerve lesion in motor axons, so the distal axons are silent *in vivo* even though the distal stumps and neuromuscular junctions remain physiologically competent to conduct action potentials and release neurotransmitter (Tsao et al., 1994; Ribchester et al., 1995; Gillingwater et al., 2002). But afferent activity, of course, originates in sensory receptors distal to the lesion: including muscle, joints and skin.

We made extracellular recordings from the tibial nerves of two terminally anaesthetised *Wld^s* mice, 5 days after cutting the sciatic nerve in the thigh. We did not observe any spontaneous action potentials or ‘injury’ discharges that might have been attributed to the nerve section itself. However, we observed brisk, multi-unit sensory discharges in the recordings from both mice, in response to a combination of cutaneous stimulation or flexion/extension of the toes, suggesting that sensory axons of modalities other than proprioceptive afferents were still functional. The multi-unit discharges were qualitatively indistinguishable from the recordings made from the tibial nerves on the unoperated, contralateral control sides (Fig. 5A, B). Thus, we concluded that axotomised sensory endings in *Wld^s* mice still respond to natural stimulation and to propagate activity in their axons, up to the lesioned region, for at least 5 days after axotomy.

The nerve recordings represented mixed sensory discharges that may have included both cutaneous and muscle afferent activity. We therefore tested for functional competence of the annulospiral endings themselves, using FM1-43 as a fluorescent reporter. Muscle stretch, which depolarises annulospiral sensory endings, facilitates up-take of amphipathic styryl dyes such as FM1-43 and RH795 (Gates et al., 1991; Bewick et al., 2005). We dissected lumbrical muscles 3–5 days after axotomy and pinned preparations of these at extended lengths in physiological saline containing 8-1-M FM1-43. Annulospiral endings in these muscles showed an increase in fluorescence compared with non-stretched muscles, suggesting that – like FM1-43 labelling of recycling synaptic vesicles in motor nerve terminals of axotomised homozygotes (Ribchester et al., 1995; Gillingwater et al., 2002) – their capacity to respond physiologically was also protected by *Wld^s* (Fig. 5C–F). Annulospiral endings of spindles in unstretched muscles did not take up the styryl dye (data not shown).

Activity does not determine differences in sensory-motor protection. If activity in the distal nerve stump were a crucial determinant of the differences in the rate of their degeneration, then abolishing or otherwise equalising the activity in sensory and motor axons should reduce or abolish these differences. Thus, having established that axotomised sensory axons and their endings remain functional *in vivo*, we next isolated pieces of sciatic or tibial nerve and maintained them in organotypic culture for 3–14 days (Bejrowski et al., 2004; Barrientos et al., 2011). Extracellular nerve recordings showed that axons in these cultures were quiescent but when stimulated electrically, they produced compound action potentials. These evoked responses declined in amplitude for up to 6 days *in vitro*, but neither the conduction velocity nor the relative refractory period of the residual axons changed significantly over this period (Franzen and Ribchester, unpublished data).

We compared sensory and motor axon degeneration morphologically in cultured explants in two ways (Fig. 6). First, we cultured explants of the saphenous nerve (purely sensory) and quadriceps muscle nerve (motor and some

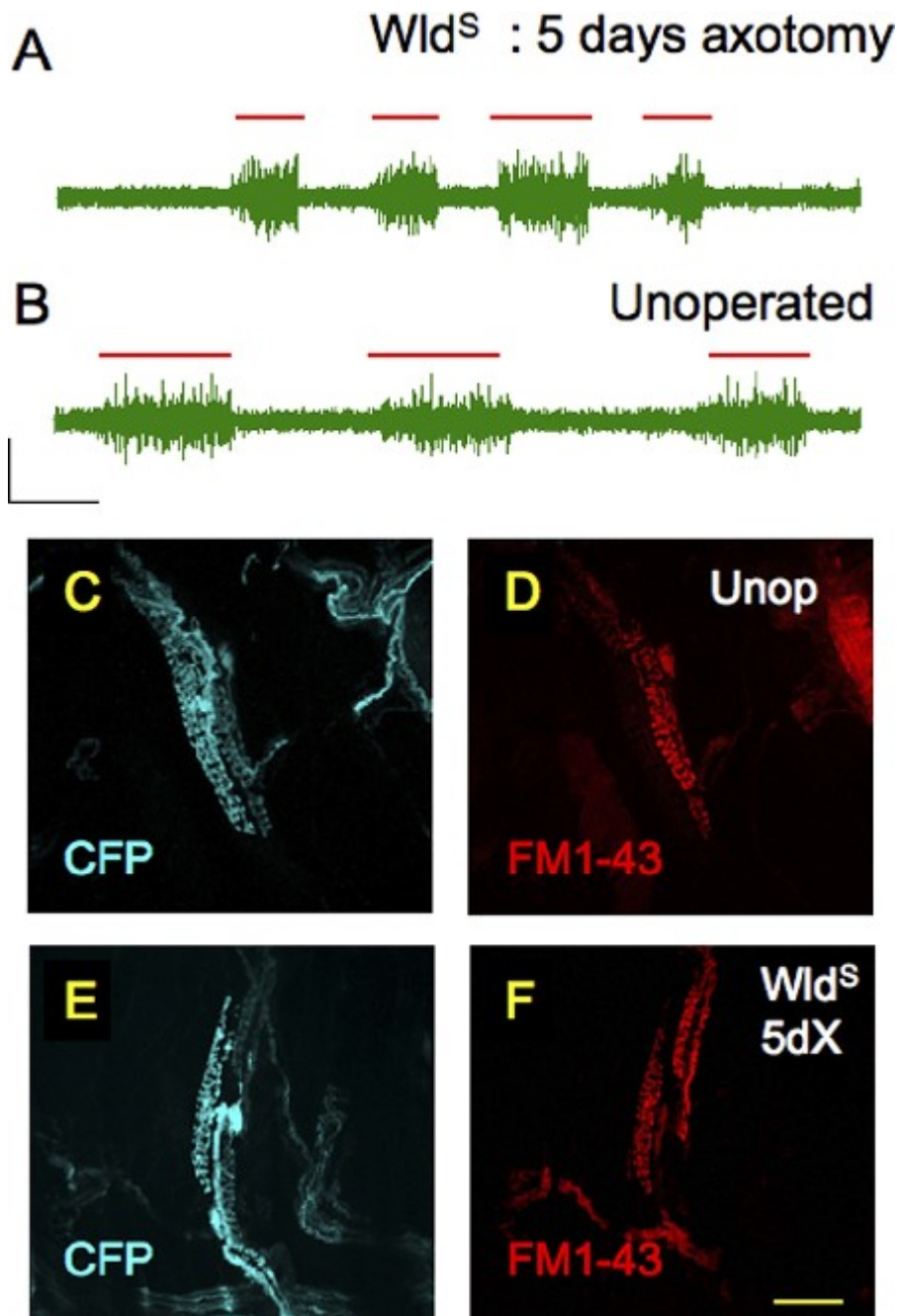


Fig. 5. Persistent sensory axons and endings are functionally competent after axotomy. Extracellular recordings showing bursts of action potentials in response to natural stimulation of cutaneous and muscle receptors combined, in a tibial nerve recording from (A) 5-d axotomised *Wld^S* mouse, (B) contralateral unoperated control tibial nerve. Touch, pressure and/or joint flexion/extension were applied at the times indicated by the red bars. (C, E) CFP fluorescence, and in the same fields (D, F) stretch-dependent loading with FM1-43fx of annulospiral endings in unoperated (C, D) 5-d axotomised DL muscle from a thy1.2 CFP:*Wld^S* mouse (E, F). Calibrations: (A), 1 mV, 400 ms; (B), 1 mV, 200 ms; (C–F) 50 μ m. For interpretation of the references to color in this figure legend, the reader is referred to the Web version of this article.

sensory) from three mice. Second, dorsal root (sensory) and ventral root (motor) explants were dissected and cultured from a further four mice. The explants were maintained in culture medium for 5–11 days. We found in all cases that sensory axons were still preserved for substantially longer than motor axons in culture (Fig. 6A–D). To quantify axonal preservation, we

first made projections of confocal z-series and counted the number of intact axons that extended over an arbitrarily chosen distance of 95 μ m or more. After 5 days of culture, 74.9 \pm 3.38% of the axons (mean \pm SEM; $n=3$ mice, 4 explants, 350 axons) in the saphenous nerve explants met this criterion, whereas only 47.9 \pm 7.88% ($n=3$ mice, 4 explants, 289 axons) were intact in the quadriceps nerves

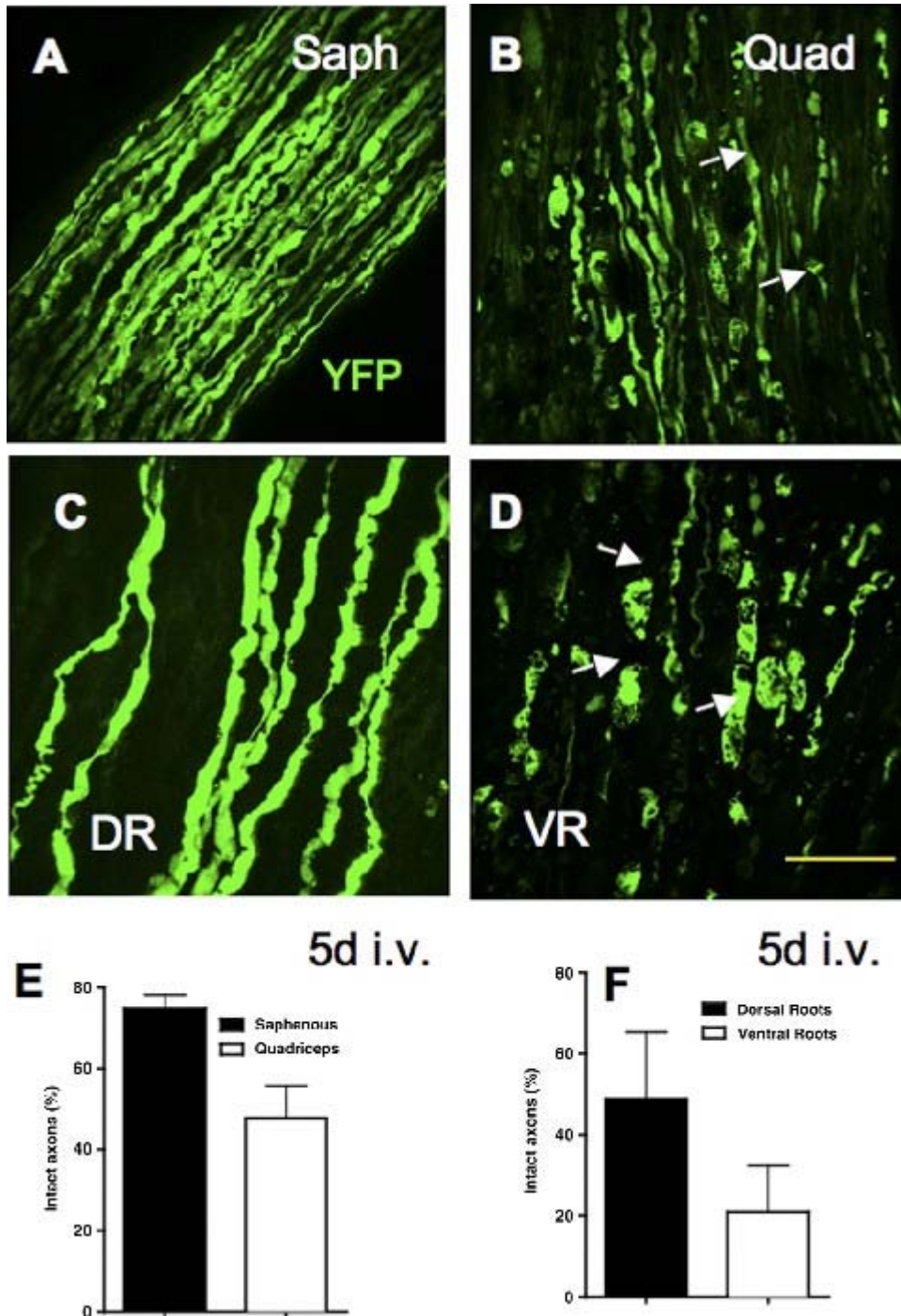


Fig. 6. Sensory-motor differences persist *in vitro* in the absence of neural activity. (A) Intact axons in the isolated saphenous nerve after 5d in culture, most axons in this field are intact and unbroken; (B) most axons in the ipsilateral quadriceps nerve were fragmented (arrows) or had degenerated after 5 d *in vitro*. (C) Intact axons after 5-d culture of dorsal roots; compared with (D), extensive fragmentation (arrows) in a ventral root explant. (E, F) Quantification of axon preservation in saphenous and quadriceps nerves (E) and dorsal and ventral roots, respectively, (F) after 5 d in culture (mean \pm SEM). Calibrations: (A, B), 100 μ m; (C, D), 50 μ m. For

interpretation of the references to color in this figure legend, the reader is referred to the Web version of this article.

from the same mice (Fig. 6E; $P < 0.05$; Mann–Whitney (mean \pm estimated SEM, 160 axons in 5 images) and $51.1 \pm$

test). In one additional pair of explants, tetrodotoxin (TTX, 5.42% (157 axons in 6 images), respectively.

2 1-M) was added and maintained in the bathing medium to Next, we explanted and cultured dorsal roots and ven- ensure complete inactivity of the axons. The axonal preser- tral roots, to compare sensory and motor axon protection vation in saphenous and quadriceps nerves was $73.8 \pm 7.8\%$ more stringently. These survived culture somewhat less well than the peripheral nerve explants but after 5 days, $48.6 \pm 16.6\%$ of the dorsal root axons were intact over a distance of 95 1-m (mean \pm SEM; $n = 4$ roots, 392 axons from two mice), whereas fewer than half the number, $21.0 \pm 11.4\%$ (4 roots, 445 axons; $P < 0.05$, t -test), were intact in the ventral root explants from the same mice (Fig. 6F). As an additional measure, we explanted roots from one thy1.2-YFPH: Wld^S mouse, in which a small subset (about 5–10%) of sensory and motor neurones express YFP (Feng et al., 2000; Beirowski et al., 2004). In these dorsal and ventral root explants, the differences between axon protection after 5 days in culture was dramatic:

$85.7 \pm 12.5\%$ of YFP-labelled dorsal root axons ($n = 72$ axons) were intact, whereas no labelled axons (0/31) re- mained intact in the ventral root explants. After 11-days culture, dorsal and ventral root explants from one addi- tional thy1.2-YFPH: Wld^S mouse, four dorsal root seg- ments contained a total of 24 YFP fluorescent axons that were intact over at least 1 mm. Several of these extended over almost the entire 5-mm length of the explant. There was only one intact YFP-positive intact axon of similar length out of five ventral root explants from the same mouse. The remaining axons had degenerated into small YFP-containing fragments.

These data confirm that substantially more sensory than motor axons are preserved following axotomy in Wld^S mice both *in vivo* and *in vitro*. The data are also consistent with previous electrophysiological recordings showing that

5 days after axotomy in Wld^S mice about half the motor axons and nerve terminals retain functional capability (Rib- chester et al., 1995; Gillingwater et al., 2002; Bridge et al.,

2009). Overall, however, the persistence of the differences in degeneration *in vitro* in the absence of activity shows that greater protection of sensory than motor axons by Wld^S is unrelated to the residual activity of their axons *in vivo*.

Nuclear levels of Wld^S protein are higher in large sen- sory neurones than motor neurones. Finally, to test whether the differences in axonal protection could be ex- plained by differences in either the expression level of Wld^S protein or its localisation, we attempted to compare Wld^S protein levels in spinal cord, dorsal root ganglia, and dorsal and ventral roots. We initially made Western blots for Wld^S protein. However, as noted by others (Beirowski et al., 2009), the results were difficult to interpret because the amount of Wld^S protein detected was very small (Oye- bode, 2009). Thus, to compare nuclear versus cytoplasmic localisation of the Wld^S protein in sensory and motor neu- rones more directly, we measured Wld^S immunofluores- cence in either whole-mounts or sections of DRG and in sections of spinal cord from Wld^S mice crossbred with thy1.2- YFP16 or thy1.2-YFPH transgenic lines (Fig. 7A, B).

Surprisingly, we found that a relatively small fraction of those cells with positive nuclear immunostaining for Wld^S also expressed YFP in the DRG of the thy1.2-YFP16: Wld^S line (compare with Table 1 in Feng et al., 2000). The fluorescent protein expression was confined mostly to the larger cells in the DRG (Fig. 7A, C). As we reported pre- viously, many of the small YFP-negative cells contained small, intense Wld^S -antibody-positive nuclear inclusions including spots, crescents, hoops and loops (Fig. 7C; see also Wilbrey et al., 2008). These may have been non- neuronal cells although Wld^S protein is not normally de- tectable in Schwann cells or other glia. Interestingly, there was little YFP fluorescence of axons or their terminals in the substantia gelatinosa of the dorsal horn of spinal cord, where the axons of many

small DRG neurones normally terminate (Fig. 7A, arrow). However, the Wld-18 immunostaining of all the large YFP-positive DRG neurones showed uniform nuclear staining. Motor neurones in the spinal cords of the same sections (thus stained under identical conditions, and imaged with identical laser and photomultiplier settings) also showed clear and uniform nuclear Wld-18 immunostaining (Figs. 7B, E and 8B).

At high magnification and image resolution (63x oil lens, 1.40 N.A) and optimal settings on the Zeiss 710 confocal microscope we also observed remarkable, distinct clusters of *Wld^S*-positive puncta in the cytoplasm of both large DRG neurones and motor neurones (Fig. 7D, F), similar to those reported previously in cultured cells transfected with *Wld^S* gene constructs but only visible with tyramide-amplification of immunostaining (Beirowski et al., 2009). Inspection of secondary antibody-only controls also showed evidence of faint punctate staining; however, the laser power and photomultiplier gain required to observe these were both much greater than for sections labelled with anti-*Wld^S* primary antibody. Thus, it appears that the *Wld^S* antibody recognises highly localised concentrations of the protein associated with a cytoplasmic compartment. The patterns of the *Wld^S*-positive clusters resemble the distribution of the ER-Golgi complex, rather than intracellular organelles such as mitochondria, and were previously shown to co-localise with markers for the ER/Golgi (Beirowski et al., 2009).

We measured the nuclear and cytoplasmic fluorescence in 30 large YFP-positive neurones in single optical sections of the DRG and compared this with the equivalent measurements in 30 large YFP-positive ventral horn neurones (presumed motor neurones) in the same physical section from one mouse spinal cord. These measurements were repeated in the same numbers of neurones in a section from a second *Wld^S* mouse. Measurements of nuclear fluorescence intensity were made with laser power, and gain and offset of the photomultiplier detectors set identically for imaging DRG neurones and spinal motor neurones (Fig. 8A, B). Some of the staining in either cytoplasmic or nuclear compartments may have represented non-specific binding of the (TRITC-conjugated) secondary antibody. However, control sections stained with the anti-rabbit secondary antibody alone (no primary Wld-18 antibody) showed a much lower level of fluorescence in the cytoplasm of neurones than in the test sections.

The data show that nuclear fluorescence of large DRG neurones was about 2.4 times brighter than in motor neurones in the same specimen (128.7 ± 6.6 arbitrary units versus 54.22 ± 2.089 ; mean \pm SEM; $P < 0.05$; Mann-Whitney; Fig. 8C). In the second mouse, the corresponding

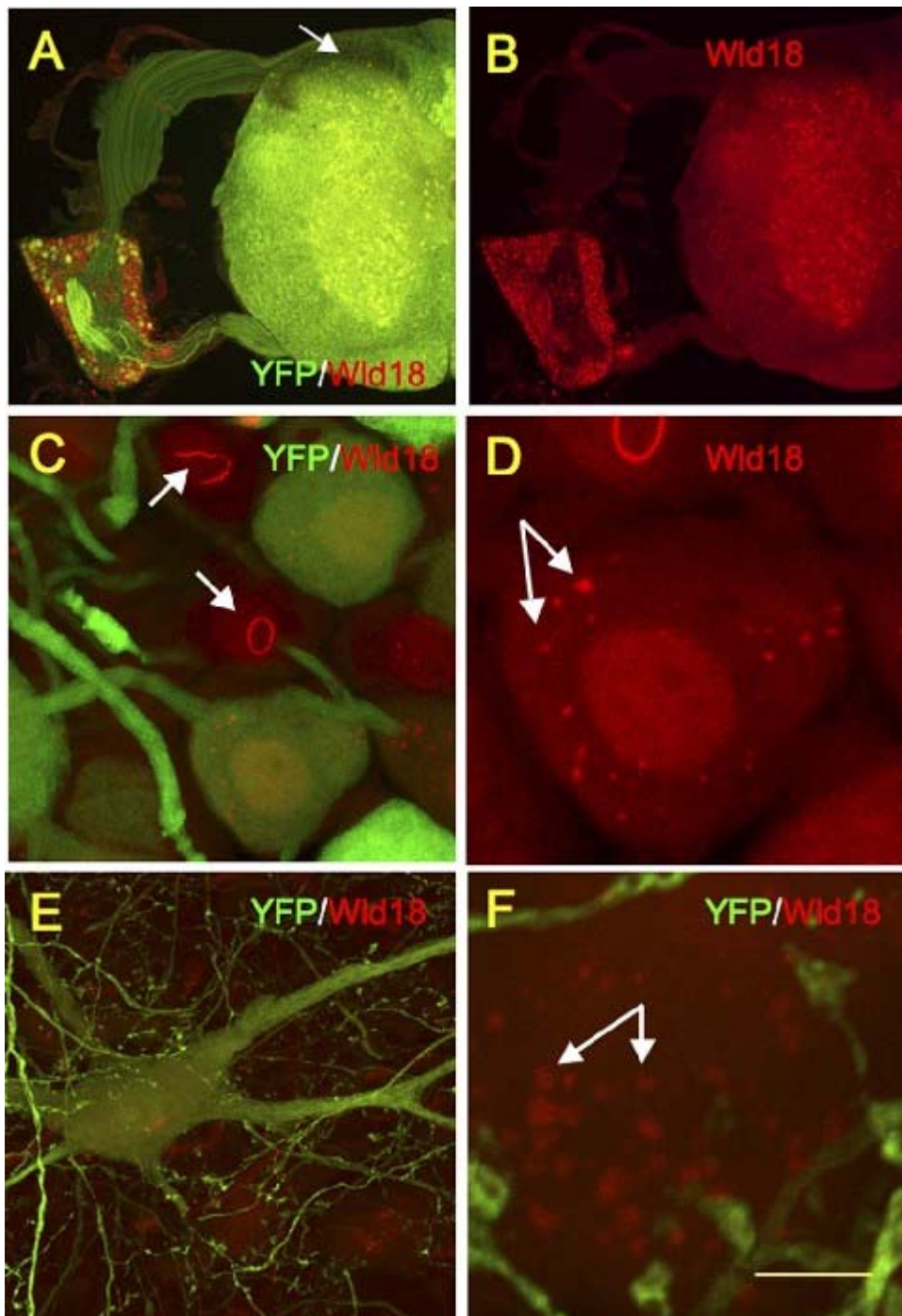


Fig. 7. Dorsal root ganglion neurones express more *Wld^S* protein than motor neurones. (A, B) Transverse section of thoracic spinal cord and DRG in a thy1.2-YFP16:*Wld^S* mouse immunostained for *Wld^S* protein (red). Note absence of YFP fluorescence in the substantia gelatinosa (arrow) and in many of the DRG neurones that strongly express *Wld^S* protein. (C) Higher power image of DRG neurones showing YFP fluorescence only in large DRG neurones with uniform nuclear staining of *Wld^S*. Note characteristic immunostaining of non-uniform nuclear inclusions positive for *Wld^S* protein in YFP-negative DRG cells (arrows). (D) Punctate staining in the cytoplasm of one of the YFP-positive large DRG neurones shown in (C) (red channel only). (E) High power image made at the same confocal microscope settings as (C, D) showing motor neurones in the ventral horn, including a YFP-positive neurone. (F) Punctate staining of cytoplasm in a YFP-negative motor neurone from a line thy1.2-YFPH:*Wld^S* mouse. Calibration: (A, B), 1 mm; (E), 20 μ m; (D, F), 10 μ m.

data were 92.39 ± 3.277 and 32.78 ± 1.194 units, respectively. Thus, the ratio of DRG nuclear fluorescence to motor neuron nuclear fluorescence in the region of the motor neurones. Subtracting motor neuron nuclear fluorescence in the same sections the background fluorescence from the two regions would

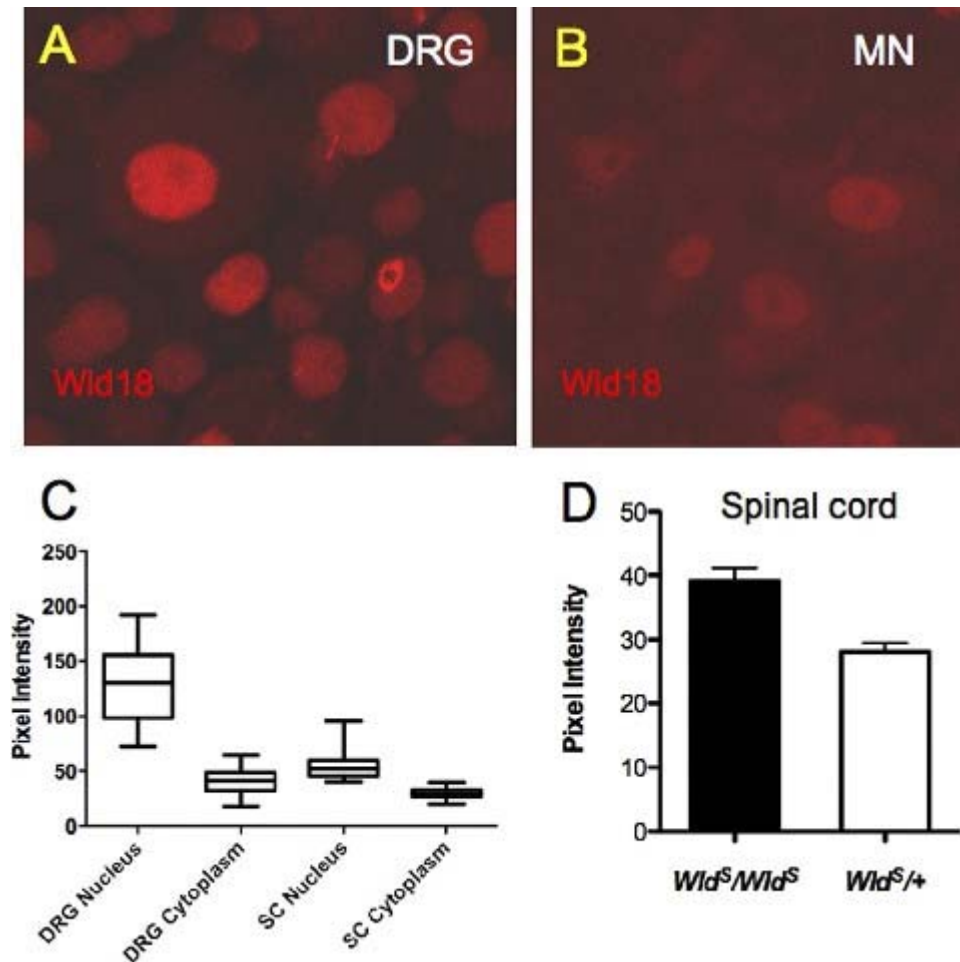


Fig. 8. *Wid^S* protein is more concentrated in DRG neurones than motor neurones. (A) DRG neurones and (B) spinal motor neurones from the same preparation, imaged at identical laser power, and photomultiplier gain and offset. Large DRG neuronal nuclei were discernibly brighter in *Wid^S* immunofluorescence than motor neurones. (C) Box-whisker plot (median, interquartile range and outliers) showing quantification of DRG neuronal brightness from one of two preparations in which nuclear and cytoplasmic intensities were measured in samples of 30 large DRG neurones and large ventral horn neurones. The DRG neuronal nuclear fluorescence was about two-fold brighter than the motor neurones ($P < 0.01$; Mann–Whitney test) but there was no significant difference comparing the brightness of the cytoplasm of the same cells. (D) Pixel brightness from four spinal cord preparations from homozygous and heterozygous *Wid^S* mice (mean \pm SEM). The settings on the confocal microscope were identical. Nuclear immunofluorescence in homozygotes was about 50% brighter than in heterozygotes ($P < 0.01$; Mann–Whitney test). For interpretation of the references to color in this figure legend, the reader is referred to the Web version of this article.

amplify the difference between sensory and motor neurones. As a reference, we also measured nuclear *Wid^S* staining in optical sections of motor neurones from heterozygous and homozygous *Wid^S* mouse spinal cord (Fig. 8D). Quantitative Western blots of brain protein extracts have previously shown that *Wid^S* heterozygotes express about half the amount of *Wid^S* protein as homozygotes (Mack et al., 2001; Conforti et al., 2009). Our quantitative analysis here shows that the fluorescence intensity of neuronal nuclei in *Wid^S* homozygotes was about 1.5 times that in heterozygotes (Fig. 8D). Thus, the simplest explanation for the difference observed between DRG

and motor neurone nuclear fluorescence in homozygotes is that DRG neurones express and concentrate in their nuclei more than twice as much *Wld^S* protein as motor neurones. We noted that the *Wld^S* immunofluorescence of the cytoplasm of some YFP-positive neurones seemed brighter than those that did not express YFP. This difference was also apparent in DRG neurones and motor neurones of thy1.2-YFPH: *Wld^S* crossbred mice. We established through careful checking of excitation and emission wavelengths in the confocal microscope that this was not due to 'bleedthrough' of YFP fluorescence; and secondary-only controls suggested it could not be due to non-specific binding of the fluorescent secondary antibody. Overall, however, we did not detect any significant difference in the absolute levels of diffuse brightness of the cytoplasm of DRG and motor neurones. We did not attempt to quantify the intensity or density of the punctate cytoplasmic staining. Wld18 antibody is highly specific for the *Wld^S* protein, and therefore produces no immunostaining of wild-type preparations, either cytologically or on Western blots (Beirowski et al., 2009; Conforti et al., 2009).

Discussion

The present study confirms the difference in the protection of sensory and motor axons by the *Wld^S* chimaeric protein in native *Wld^S* mutant mice reported previously and extends this finding by showing qualitatively and quantitatively substantial differences in protection of sensory and motor axon terminals. Sensory endings are preserved at least twice as long as motor nerve terminals following axotomy in *Wld^S* mice and the protection of sensory axons and their endings is hardly weakened at all in *Wld^S /+* heterozygotes, nor is it dramatically affected by aging. In contrast, the protection of motor nerve terminals is extremely sensitive to *Wld^S* 'gene-dose' and diminishes progressively with age (Gillingwater et al., 2002; Beirowski et al., 2009; Wong et al., 2009). We have ruled out here at least one plausible explanation: that the differences in protection might be due to differences in ongoing evoked sensory and motor activity. Sensory axons still persisted longer than motor axons *in vitro*, even when all possible activity was abolished with TTX. We did find evidence for an effect of nerve branching since, at least in older homozygous mice, the amount of protection of γ -motor axons and their endings was greater than that of α -motor axons and their terminals but less than that of sensory axons and their annulospiral endings innervating muscle spindles. By contrast, we did not detect any difference in the protection of the γ -innervation of spindles in wild-type and heterozygous *Wld^S* mice. Finally, immunofluorescent staining for *Wld^S* protein was more than twice as intense in the nuclei of DRG neurones than motor neurones in the same mice, and this was greater than the difference in measurements comparing nuclear *Wld^S*-immunofluorescence in homozygotes and heterozygotes.

The site and mechanism of *Wld^S* action

In common with previous studies (Mack et al., 2001; Beirowski et al., 2009), we were unable to detect substantial amounts of *Wld^S* protein concentration in the cytoplasm of axons in peripheral nerves or dorsal root or ventral roots, using either immunocytochemical staining or Western blotting. These methods are evidently just not sensitive enough to detect levels of *Wld^S* protein that are nevertheless more than sufficient to confer a strong axon-protective phenotype *in vivo* and *in vitro* (Beirowski et al., 2009). However, we detected *Wld^S*-positive punctate inclusions in both sensory and motor neurone cell bodies, consistent with targeting of the protein to an intracellular compartment possibly the ER-Golgi complex (Beirowski et al., 2009) although differences in fluorescence intensity were not discernible in these puncta. Of course, it is by no means certain that a strong difference in the concentration of nuclear *Wld^S* in sensory or motor neurones reflects also a sufficient difference in the cytoplasmic levels to account for the difference in sensory-motor protective phenotype (Beirowski et al., 2009; Babetto et al., 2010). However, the differences in nuclear expression levels apparent from measurements of nuclear immunofluorescence in homozygotes and heterozygotes, which does correlate with the

strength of the phenotype in motor neurones (Mack et al., 2001; Wong et al., 2009), are consistent with differences in cytoplasmic levels of *Wld^S* in motor and sensory axons at the site of action necessary for axon protection. Interestingly, sensory axon protection in heterozygotes was almost as strong as in homozygotes; but the fluorescence intensity differences between DRG neuronal nuclear *Wld^S* immunofluorescence and that of motor neurones were greater than the homozygous-heterozygous difference. Taken together with the observed relationship between *Wld^S* protein level and axon protection, based on studies of transgenic mice with different expression levels of *Wld^S* protein (Mack et al., 2001), this suggests that the expression level of *Wld^S* protein in sensory neurones, even in heterozygotes, is still above the level required to saturate its protective effect. Differences in the expression levels of *Wld^S* protein in sensory and motor neurones therefore remain the most likely explanation for the differences in sensory-motor axon protection. More complex explanations, such as cell-type specific differences in set-point or gain of the molecular amplifiers in the intracellular signalling pathways that mediate the *Wld^S*-effect cannot be ruled out. The data also indicate the importance of exercising caution, by establishing the level of *Wld^S* expression in neuronal populations and sub-types before making deductions about the strength, selectivity, 'gene-dose' or age-dependence of *Wld^S*-induced axonal or terminal protection phenotype in different neurones or their component parts (Wilbrey et al., 2008; Wright et al., 2010).

Activity independence of axonal protection

Synaptic degeneration can be mitigated by environmental, activity-inducing influences (Caston et al., 1999; Hultsch et al., 1999; Selkoe, 2002; Swaab et al., 2002; Saxena and Caroni, 2007). However, other studies suggest that inactivity slows axonal degeneration (Kapoor et al., 2003; Hains et al., 2004; Iwata et al., 2004).

Wld^S mouse muscles become paralysed *in vivo* after axotomy because, of course, their axons are disconnected from the CNS. Clinically, axotomised limbs in *Wld^S* mice show flaccid paralysis that is consistent with a complete absence of any spontaneous or 'injury'-induced discharges. However, NMJs remain physiologically competent for several days: compound action potentials and evoked neuromuscular synaptic responses can still be evoked by stimulation of the distal stump for up to 2 weeks after nerve injury (Tsao et al., 1994; Gillingwater et al., 2002). In contrast, axotomised peripheral sensory axons, of course, remain connected to their normal source of endogenous excitation, that is, their receptive endings in skin, joints, muscle and other tissue. The recordings we made *in vivo* in the present study show that natural stimuli applied by even passive movement of the hind limbs still produce afferent action potentials (notwithstanding that the signals produced reach only as far as the site of the peripheral nerve lesion). There was no evidence for any residual spontaneous activity in the axotomised nerve recordings (Fig. 5). The present data convincingly show that equalising activity in sensory and motor axons *in vitro* did not abolish their difference in resistance to degeneration in *Wld^S* mice *in vivo*. Thus, differences in residual activity do not explain the differences in protection of sensory and motor axons.

Translation of protection to models of disease

Several attempts have been made to transfer the neuroprotective benefits of *Wld^S* expression to animal models of neurodegenerative disease, with variable success. Cross-breeding *Wld^S* mice with models of peripheral neuropathy or axonopathy disease mitigates the onset and progression of disease signs (Wang et al., 2001, 2002; Ferri et al., 2003; Samsam et al., 2003; Watanabe et al., 2007; Meyer zu Horste et al., 2011). However, not all models of neurodegeneration are protected by co-expression of *Wld^S* (Vande Velde et al., 2004; Fischer et al., 2005; Kariya et al., 2009). The reasons for failure of neuroprotection in these instances are unclear but since motor nerve terminals in *Wld^S* mice and their transgenic equivalents lose their capacity to inhibit degeneration of motor nerve terminals as the mice age (Gillingwater et al., 2002; Adalbert et al., 2005), mouse models with a late onset of disease are less likely to benefit or be protected from co-expression of the protective gene.

Interestingly, in the present study, protection of sensory axons and their endings showed a much weaker dependence on mouse age. The age-dependence of the protective phenotype is also much less in transgenic mice in which *Wld^S* protein (or Nmnat-1 activity) was targeted to axons, even at very low expression levels (Beirowski et al., 2009; Babetto et al., 2010). Expression level of the mutant protein is another important factor in determining the strength of the *Wld^S* phenotype (Mack et al., 2001; Gillingwater et al., 2002). Axon terminals may be even more sensitive to the *Wld^S* 'gene-dose'. For instance, while axons are protected for at least 3 days after nerve injury in heterozygous *Wld^S* mice, which show about half the expression level of the mutant protein, the rate of degeneration of motor nerve terminals in *Wld^S* heterozygotes is almost indistinguishable from that in wild-type mice (Wong et al., 2009). Axons and their terminals in the CNS are also protected only half as strongly in *Wld^S* heterozygotes compared with homozygotes (Wright et al., 2010).

These findings, together, suggest that re-evaluation of the potential protective benefits of *Wld^S* would be worthwhile in those models of axonopathy, synaptopathy or other forms of neurodegenerative disease where co-expression of the natural mutant protein failed. For instance, mimicry of the *Wld^S* phenotype may be particularly effective and beneficial in the treatment of sensory neuropathies such as gracile axonal dystrophy (Kikuchi et al., 1990; Oda et al., 1992; Mi et al., 2005) or neurotoxic damage by chemotherapeutic agents such as cisplatin or taxol used in the treatment of cancer (von Schlippe et al., 2001; Wang et al., 2002; Watanabe et al., 2007). Adjusting the levels of expression and the localisation of expression of *Wld^S* protein in specific neuronal subtypes, or selective mimicry of the down-stream signalling mechanisms in those sub-types, could yield more substantial neuroprotective benefits for specific sensory or motor neuronopathies than achieved previously. It is noteworthy that explants or dissociated neurones from DRG are routinely used to assay the strength of axon protection by *Wld^S* (Buckmaster et al., 1995; Wang et al., 2001; Araki et al., 2004; Conforti et al., 2007, 2009).

Conclusions

We have confirmed that sensory axons are better protected than motor axons following nerve injury in *Wld^S* mutant mice. We extended this observation first, by showing that the differences extend to annulospiral sensory endings of muscle spindles compared with skeletomotor nerve terminals. The differences do not correlate with predicted differences in the residual activity of axotomised distal sensory and motor axons but rather, with differences in the *Wld^S* protein expression level detected in sensory and motor neurones.

Acknowledgements

We thank Professor Mike Ludwig for assistance with extracellular nerve recordings and Dr. Michael Coleman for the generous gift of Wld18 antibody. Supported by MRC Studentship to O.R.O.O. and Project Grants from the Motor Neuron Disease Association (MNDA) and MND Scotland.

References

Adalbert R, Gillingwater TH, Haley JE, Bridge K, Beirowski B, Berek L, Wagner D, Grumme D, Thomson D, Celik A, Addicks K, Ribchester RR, Coleman MP (2005) A rat model of slow Wallerian degeneration (WldS) with improved preservation of neuromuscular synapses. *Eur J Neurosci* 21:271–277.

Araki T, Sasaki Y, Milbrandt J (2004) Increased nuclear NAD biosynthesis and SIRT1 activation prevent axonal degeneration. *Science* 305:1010–1013.

- Babetto E, Beirowski B, Janeckova L, Brown R, Gilley J, Thomson D, Ribchester RR, Coleman MP (2010) Targeting NMNAT1 to axons and synapses transforms its neuroprotective potency in vivo. *J Neurosci* 30:13291–13304.
- Barker D, Emonet-Dénand F, Harker DW, Jami L, Laporte Y (1977) Types of intra- and extrafusal muscle fibre innervated by dynamic skeleto-fusimotor axons in cat peroneus brevis and tenuissimus muscles, as determined by the glycogen-depletion method. *J Physiol* 266:713–726.
- Barrientos SA, Martinez NW, Yoo S, Jara JS, Zamorano S, Hetz C, Twiss JL, Alvarez J, Court FA (2011) Axonal degeneration is mediated by the mitochondrial permeability transition pore. *J Neurosci* 31:966–978.
- Beirowski B, Adalbert R, Wagner D, Grumme DS, Addicks K, Ribchester RR, Coleman MP (2005) The progressive nature of Wallerian degeneration in wild-type and slow Wallerian degeneration (Wlds) nerves. *BMC Neurosci* 6:6.
- Beirowski B, Babetto E, Gilley J, Mazzola F, Conforti L, Janeckova L, Magni G, Ribchester RR, Coleman MP (2009) Non-nuclear Wld(S) determines its neuroprotective efficacy for axons and synapses in vivo. *J Neurosci* 29:653–668.
- Beirowski B, Berek L, Adalbert R, Wagner D, Grumme DS, Addicks K, Ribchester RR, Coleman MP (2004) Quantitative and qualitative analysis of Wallerian degeneration using restricted axonal labelling in YFP-H mice. *J Neurosci Methods* 134:23–35.
- Bewick GS, Reid B, Richardson C, Banks RW (2005) Autogenic modulation of mechanoreceptor excitability by glutamate release from synaptic-like vesicles: evidence from the rat muscle spindle primary sensory ending. *J Physiol* 562:381–394.
- Bridge KE, Berg N, Adalbert R, Babetto E, Dias T, Spillantini MG, Ribchester RR, Coleman MP (2009) Late onset distal axonal swelling in YFP-H transgenic mice. *Neurobiol Aging* 30:309–321.
- Brown MC, Perry VH, Hunt SP, Lapper SR (1994) Further studies on motor and sensory nerve regeneration in mice with delayed Wallerian degeneration. *Eur J Neurosci* 6:420–428.
- Buckmaster EA, Perry VH, Brown MC (1995) The rate of Wallerian degeneration in cultured neurons from wild type and C57BL/WldS mice depends on time in culture and may be extended in the presence of elevated K⁺ levels. *Eur J Neurosci* 7:1596–1602.
- Caston J, Devulder B, Jouen F, Lalonde R, Delhaye-Bouchaud N, Mariani J (1999) Role of an enriched environment on the restoration of behavioral deficits in Lurcher mutant mice. *Dev Psychobiol* 35:291–303.
- Coleman MP, Conforti L, Buckmaster EA, Tarlton A, Ewing RM, Brown MC, Lyon MF, Perry VH (1998) An 85-kb tandem triplication in the slow Wallerian degeneration (Wlds) mouse. *Proc Natl Acad Sci U S A* 95:9985–9990.
- Coleman MP, Freeman MR (2010) Wallerian degeneration, wld(s), and nmnat. *Annu Rev Neurosci* 33:245–267.
- Conforti L, Fang G, Beirowski B, Wang MS, Sorci L, Asress S, Adalbert R, Silva A, Bridge K, Huang XP, Magni G, Glass JD, Coleman MP (2007) NAD(+) and axon degeneration revisited: Nmnat1 cannot substitute for Wld(S) to delay Wallerian degeneration. *Cell Death Differ* 14:116–127.
- Conforti L, Tarlton A, Mack TG, Mi W, Buckmaster EA, Wagner D, Perry VH, Coleman MP (2000) A Ufd2/D4Cole1e chimeric protein and overexpression of Rbp7 in the slow Wallerian degeneration (Wlds) mouse. *Proc Natl Acad Sci U S A* 97:11377–11382.
- Conforti L, Wilbrey A, Morreale G, Janeckova L, Beirowski B, Adalbert R, Mazzola F, Di Stefano M, Hartley R, Babetto E, Smith T, Gilley J, Billington RA, Genazzani AA, Ribchester RR, Magni G, Coleman M (2009) Wld S protein requires Nmnat activity and a short N-terminal sequence to protect axons in mice. *J Cell Biol* 184:491–500.

- David G, Nguyen K, Barrett EF (2007) Early vulnerability to ischemia/ reperfusion injury in motor terminals innervating fast muscles of SOD1-G93A mice. *Exp Neurol* 204:411– 420.
- Desaki J, Ezaki T, Nishida N (2010) Fine structural study of the innervation of muscle spindles in the internal oblique muscle of the abdominal wall in the adult mouse. *J Electron Microsc (Tokyo)* 59:243–250.
- Feng G, Mellor RH, Bernstein M, Keller-Peck C, Nguyen QT, Wallace M, Nerbonne JM, Lichtman JW, Sanes JR (2000) Imaging neuronal subsets in transgenic mice expressing multiple spectral variants of GFP. *Neuron* 28:41–51.
- Ferri A, Sanes JR, Coleman MP, Cunningham JM, Kato AC (2003) Inhibiting axon degeneration and synapse loss attenuates apoptosis and disease progression in a mouse model of motoneuron disease. *Curr Biol* 13:669 – 673.
- Fischer LR, Culver DG, Davis AA, Tennant P, Wang M, Coleman M, Asress S, Adalbert R, Alexander GM, Glass JD (2005) The WldS gene modestly prolongs survival in the SOD1G93A fALS mouse. *Neurobiol Dis* 19:293–300.
- Fischer LR, Culver DG, Tennant P, Davis AA, Wang M, Castellano- Sanchez A, Khan J, Polak MA, Glass JD (2004) Amyotrophic lateral sclerosis is a distal axonopathy: evidence in mice and man. *Exp Neurol* 185:232–240.
- Forero DA, Casadesus G, Perry G, Arboleda H (2006) Synaptic dysfunction and oxidative stress in Alzheimer's disease: emerging mechanisms. *J Cell Mol Med* 10:796 – 805.
- Frey D, Schneider C, Xu L, Borg J, Spooren W, Caroni P (2000) Early and selective loss of neuromuscular synapse subtypes with low sprouting competence in motoneuron diseases. *J Neurosci* 20:2534 –2542.
- Gates HJ, Ridge RM, Rowleson A (1991) Motor units of the fourth deep lumbrical muscle of the adult rat: isometric contractions and fibre type compositions. *J Physiol* 443:193–215.
- Gilley J, Coleman MP (2010) Endogenous Nmnat2 is an essential survival factor for maintenance of healthy axons. *PLoS Biol* 8:e1000300.
- Gillingwater TH, Ingham CA, Coleman MP, Ribchester RR (2003) Ultrastructural correlates of synapse withdrawal at axotomized neuromuscular junctions in mutant and transgenic mice expressing the Wld gene. *J Anat* 203:265–276.
- Gillingwater TH, Ribchester RR (2001) Compartmental neurodegeneration and synaptic plasticity in the Wld(s) mutant mouse. *J Physiol* 534:627– 639.
- Gillingwater TH, Thomson D, Mack TG, Soffin EM, Mattison RJ, Coleman MP, Ribchester RR (2002) Age-dependent synapse withdrawal at axotomized neuromuscular junctions in Wld(s) mutant and Ube4b/Nmnat transgenic mice. *J Physiol* 543:739 –755.
- Hains BC, Saab CY, Lo AC, Waxman SG (2004) Sodium channel blockade with phenytoin protects spinal cord axons, enhances axonal conduction, and improves functional motor recovery after contusion SCI. *Exp Neurol* 188:365–377.
- Hoopfer ED, McLaughlin T, Watts RJ, Schuldiner O, O'Leary DD, Luo L (2006) Wlds protection distinguishes axon degeneration following injury from naturally occurring developmental pruning. *Neuron* 50:883– 895.
- Hultsch DF, Hertzog C, Small BJ, Dixon RA (1999) Use it or lose it: engaged lifestyle as a buffer of cognitive decline in aging? *Psychol Aging* 14:245–263.

Iwata A, Stys PK, Wolf JA, Chen XH, Taylor AG, Meaney DF, Smith DH (2004) Traumatic axonal injury induces proteolytic cleavage of the voltage-gated sodium channels modulated by tetrodotoxin and protease inhibitors. *J Neurosci* 24:4605–4613.

Kapoor R, Davies M, Blaker PA, Hall SM, Smith KJ (2003) Blockers of sodium and calcium entry protect axons from nitric oxide-mediated degeneration. *Ann Neurol* 53:174–180.

Kariya S, Mauricio R, Dai Y, Monani UR (2009) The neuroprotective factor Wld(s) fails to mitigate distal axonal and neuromuscular junction (NMJ) defects in mouse models of spinal muscular atrophy. *Neurosci Lett* 449:246–251.

Kikuchi T, Mukoyama M, Yamazaki K, Moriya H (1990) Axonal degeneration of ascending sensory neurons in gracile axonal dystrophy mutant mouse. *Acta Neuropathol* 80:145–151.

Kucera J, Walro JM, Reichler J (1991) Neural organization of spindles in three hindlimb muscles of the rat. *Am J Anat* 190:74–88.

Lin YC, Koleske AJ (2010) Mechanisms of synapse and dendrite maintenance and their disruption in psychiatric and neurodegenerative disorders. *Annu Rev Neurosci* 33:349–378.

Lu J, Tapia JC, White OL, Lichtman JW (2009) The interscutularis muscle connectome. *PLoS Biol* 7:e32.

Lunn ER, Perry VH, Brown MC, Rosen H, Gordon S (1989) Absence of Wallerian degeneration does not hinder regeneration in peripheral nerve. *Eur J Neurosci* 1:27–33.

Lyon MF, Ogunkolade BW, Brown MC, Atherton DJ, Perry VH (1993) A gene affecting Wallerian nerve degeneration maps distally on mouse chromosome 4. *Proc Natl Acad Sci U S A* 90:9717–9720. MacDonald JM, Beach MG, Porpiglia E, Sheehan AE, Watts RJ, Freeman MR (2006) The *Drosophila* cell corpse engulfment receptor Draper mediates glial clearance of severed axons. *Neuron* 50:869–881.

Mack TG, Reiner M, Beirowski B, Mi W, Emanuelli M, Wagner D, Thomson D, Gillingwater T, Court F, Conforti L, Fernando FS, Tarlton A, Andressen C, Addicks K, Magni G, Ribchester RR, Perry VH, Coleman MP (2001) Wallerian degeneration of injured axons and synapses is delayed by a *Ube4b/Nmnat* chimeric gene. *Nat Neurosci* 4:1199–1206.

Martin SM, O'Brien GS, Portera-Cailliau C, Sagasti A (2010) Wallerian degeneration of zebrafish trigeminal axons in the skin is required for regeneration and developmental pruning. *Development* 137:3985–3994.

Meyer zu Horste G, Miesbach TA, Muller JI, Fledrich R, Stassart RM, Kieseier BC, Coleman MP, Sereda MW (2011) The *Wlds* transgene reduces axon loss in a Charcot-Marie-Tooth disease 1A rat model and nicotinamide delays post-traumatic axonal degeneration. *Neurobiol Dis* 42:1–8.

Mi W, Beirowski B, Gillingwater TH, Adalbert R, Wagner D, Grumme D, Osaka H, Conforti L, Arnhold S, Addicks K, Wada K, Ribchester RR, Coleman MP (2005) The slow Wallerian degeneration gene, *Wlds*, inhibits axonal spheroid pathology in gracile axonal dystrophy mice. *Brain* 128:405–416.

Miledi R, Slater CR (1968) Electrophysiology and electron-microscopy of rat neuromuscular junctions after nerve degeneration. *Proc R Soc Lond B Biol Sci* 169:289–306.

Oda K, Yamazaki K, Miura H, Shibasaki H, Kikuchi T (1992) Dying back type axonal degeneration of sensory nerve terminals in muscle spindles of the gracile axonal dystrophy (GAD) mutant mouse. *Neuropathol Appl Neurobiol* 18:265–281.

Ovalle WK Jr. (1972) Fine structure of rat intrafusal muscle fibers. The equatorial region. *J Cell Biol* 52:382–396. Oyebo ORO (2009) Protection of neuromuscular sensory endings by the *Wlds* gene. University of Edinburgh PhD Thesis.

- Porayko O, Smith RS (1968) Morphology of muscle spindles in the rat. *Experientia* 24:588–589.
- Ribchester RR, Tsao JW, Barry JA, Asgari-Jirhandeh N, Perry VH, Brown MC (1995) Persistence of neuromuscular junctions after axotomy in mice with slow Wallerian degeneration (C57BL/WldS). *Eur J Neurosci* 7:1641–1650.
- Samsam M, Mi W, Wessig C, Zielasek J, Toyka KV, Coleman MP, Martini R (2003) The WldS mutation delays robust loss of motor and sensory axons in a genetic model for myelin-related axonopathy. *J Neurosci* 23:2833–2839.
- Saxena S, Caroni P (2007) Mechanisms of axon degeneration: from development to disease. *Prog Neurobiol* 83:174–191.
- Schaefer AM, Sanes JR, Lichtman JW (2005) A compensatory sub-population of motor neurons in a mouse model of amyotrophic lateral sclerosis. *J Comp Neurol* 490:209–219.
- Selkoe DJ (2002) Alzheimer's disease is a synaptic failure. *Science* 298:789–791.
- Slater CR (1966) Time course of failure of neuromuscular transmission after motor nerve section. *Nature* 209:305–306.
- Swaab DF, Dubelaar EJ, Hofman MA, Scherder EJ, van Someren EJ, Verwer RW (2002) Brain aging and Alzheimer's disease; use it or lose it. *Prog Brain Res* 138:343–373.
- Tourtellotte WG, Keller-Peck C, Milbrandt J, Kucera J (2001) The transcription factor Egr3 modulates sensory axon-myotube interactions during muscle spindle morphogenesis. *Dev Biol* 232: 388–399.
- Tsao JW, Brown MC, Carden MJ, McLean WG, Perry VH (1994) Loss of the compound action potential: an electrophysiological, biochemical and morphological study of early events in axonal degeneration in the C57BL/Ola mouse. *Eur J Neurosci* 6:516–524.
- Vande Velde C, Garcia ML, Yin X, Trapp BD, Cleveland DW (2004) The neuroprotective factor WldS does not attenuate mutant SOD1-mediated motor neuron disease. *Neuromolecular Med* 5:193–203.
- von Schlippe M, Fowler CJ, Harland SJ (2001) Cisplatin neurotoxicity in the treatment of metastatic germ cell tumour: time course and prognosis. *Br J Cancer* 85:823–826.
- Wang MS, Davis AA, Culver DG, Glass JD (2002) WldS mice are resistant to paclitaxel (taxol) neuropathy. *Ann Neurol* 52:442–447.
- Wang MS, Fang G, Culver DG, Davis AA, Rich MM, Glass JD (2001) The WldS protein protects against axonal degeneration: a model of gene therapy for peripheral neuropathy. *Ann Neurol* 50:773–779.
- Watanabe M, Tsukiyama T, Hatakeyama S (2007) Protection of vincristine-induced neuropathy by WldS expression and the independence of the activity of Nmnat1. *Neurosci Lett* 411:228–232.
- Wilbrey AL, Haley JE, Wishart TM, Conforti L, Morreale G, Beirowski B, Babetto E, Adalbert R, Gillingwater TH, Smith T, Wyllie DJ, Ribchester RR, Coleman MP (2008) VCP binding influences intracellular distribution of the slow Wallerian degeneration protein, Wld(S). *Mol Cell Neurosci* 38:325–340.
- Winlow W, Usherwood PN (1975) Ultrastructural studies of normal and degenerating mouse neuromuscular junctions. *J Neurocytol* 4:377–394.
- Winlow W, Usherwood PN (1976) Electrophysiological studies of normal and degenerating mouse neuromuscular junctions. *Brain Res* 110:447–461.

Wong F, Fan L, Wells S, Hartley R, Mackenzie FE, Oyebode O, Brown R, Thomson D, Coleman MP, Blanco G, Ribchester RR (2009) Axonal and neuromuscular synaptic phenotypes in Wld(S), SOD1(G93A) and ostes mutant mice identified by fiber-optic con- focal microendoscopy. *Mol Cell Neurosci* 42:296–307.

Wright AK, Wishart TM, Ingham CA, Gillingwater TH (2010) Synaptic protection in the brain of WldS mice occurs independently of age but is sensitive to gene-dose. *PLoS One* 5:e15108.

Appendix

Supplementary data